

# Increase of Wave Height Due to Transition in Wind Direction - Example: Rijeka Bay

---

Lončar, Goran; Šreng, Željko; Miličević, Hanna; Ostojić, Sanja

Source / Izvornik: **Electronic journal of the Faculty of Civil Engineering Osijek - e-GFOS, 2019, 18, 57 - 70**

**Journal article, Published version**

**Rad u časopisu, Objavljena verzija rada (izdavačev PDF)**

<https://doi.org/10.13167/2019.18.6>

Permanent link / Trajna poveznica: <https://urn.nsk.hr/urn:nbn:hr:237:486241>

Rights / Prava: [In copyright](#)/[Zaštićeno autorskim pravom.](#)

Download date / Datum preuzimanja: **2024-09-19**

Repository / Repozitorij:

[Repository of the Faculty of Civil Engineering,  
University of Zagreb](#)





## INCREASE OF WAVE HEIGHT DUE TO TRANSITION IN WIND DIRECTION – EXAMPLE: RIJEKA BAY

*Scientific paper / Znanstveni rad*

*(Received: 21 March 2019; accepted: 04 June 2019)*

### **Goran Lončar**

*University of Zagreb, Faculty of Civil Engineering, Full Professor*

*Corresponding author: goran.loncar@grad.unizg.hr*

### **Željko Šreng**

*University of Osijek, Faculty of Civil Engineering and Architecture Osijek, Ph.D.*

### **Hanna Miličević**

*University of Zagreb, Faculty of Civil Engineering, Student*

### **Sanja Ostojić**

*University of Zagreb, Faculty of Civil Engineering, Student*

**Abstract:** Surface wind wave dynamics were analyzed during wind transition from the third to the fourth quadrant, with the transition from Sirocco to Libeccio used as an example. This research is focused on the deep-water area in front of the Rijeka port. The analyses utilized a numerical model for wave generation, covering the entire Adriatic basin. Numerical simulations were conducted for relevant situations during the period 1998-2001. The numerical model was forced by the wind field obtained from the Aladin-HR atmospheric model. Numerical simulations were conducted in two steps, initially using hypothetical scenarios with homogenous and stationary wind fields, followed by simulations based on nonstationary wind fields from the Aladin-HR atmospheric model. The first step was used to confirm the hypothesis that significant wave heights rise during the transition of wind direction in the analyzed area. Model simulations in step two verified the assumption that the observed phenomenon can also occur in real atmospheric conditions. The results of the model simulations indicate the onset of a significant wave height increase during the transition of wind direction from the SSE to SW in a wider area that includes Kvarner and Rijeka bay. The increase in wind velocity results in a more noticeable significant wave height maximum.

**Keywords:** significant wave height, numerical model, Rijeka Bay, model Aladin

## RAST VALNIH VISINA PRI TRANZICIJI SMJERA VJETRA – PRIMJER RIJEČKOG ZALJEVA

**Sažetak:** Analizirana je dinamika valnih visina tijekom tranzicije smjera vjetra iz trećeg u četvrti kvadrant, poglavito juga u lebić. Područje istraživanja fokusirano je na dubokovodno područje ispred luke Rijeka. U analizama je primijenjen numerički model valnog generiranja s obuhvatom cijelog jadranskog bazena. Numeričke simulacije su provedene za relevantne situacije tijekom razdoblja 1998. - 2001. godine. Numerički model je forsiran poljem vjetra dobivenim iz atmosferskog modela Aladin/HR. Numeričke simulacije provedene su u dva koraka, inicijalno korištenjem hipotetskih scenarija s djelovanjem homogenog i stacionarnog polja vjetra te nastavno primjenom nestacionarnog polja vjetra iz atmosferskog modela Aladin/Hr. Prvom koraku istraživanja cilj je potvrditi hipoteze o rastu izrazitih valnih visina tijekom tranzicije smjera vjetra u analiziranom području. Modelske simulacije u drugom koraku potvrđuju pretpostavku da uočena fenomenologija može nastupiti i u realnim atmosferskim uvjetima. Rezultati modelskih simulacija ukazuju na pojavu ekstrema  $H_s$  u situacijama kada tranzicija smjera vjetra iz JJI u JZ nastupa u širem području koje uključuje i Kvarner i riječki zaljev. Veća brzina vjetra rezultira izraženijim ekstremom  $H_s$ .

**Cljučne riječi:** izrazita valna visina, numerički model, riječki zaljev, model Aladin

Lončar, G, Šreng, Ž, Miličević, H, Ostojić, S



## 1 INTRODUCTION

Kvarner (Figure 1) is a part of the Adriatic Sea, located between the Istrian and Vinodol-Velebit coast. Kvarner Bay is divided into the Rijeka Bay, Kvarnerić, Velebit channel, Vinodol channel and Kvarner in the narrow sense, by the series of islands Cres-Lošinj and Krk-Rab-Pag. In the north it is bordered by the Vela Vrata and on the south by the line from the Kamenjak to the Premuda Island. The Bay of Rijeka is the inner part of the Kvarner Bay and covers 450 km<sup>2</sup>. The Vela Vrata and Srednja Vrata connect it with the open sea. Its maximum depth is 67 m. Tides have an amplitude of up to 0.8 m and its average salinity is 37.5 PSU [1]. In the Bay of Bakar, at the mouth of the Rječina river and along the coast of Opatija, the sea is less saline and colder due to the appearance of submarine springs. Its color is extremely blue, and its transparency is up to 20 m [1]. The dominant wind is the Bora (often of hurricane strength) followed by the Sirocco and Mistral.

The Adriatic Sea is a semi-enclosed sea with limited fetches. The occurrence of fully developed wind waves is unusual, however, instrument measurements show that during strong gale force winds with longer fetches, waves of respectable dimensions may be developed in the open sea of the Adriatic Sea area [2]. The absolute maximum wave height in the Adriatic Sea was measured in the north Adriatic ( $H_{\max} = 10.8$  m). The expected value of wave height for a return period of 100 years in the Adriatic is about 14 m [3]. Measurements of wind-generated surface waves in the eastern part of the Adriatic Sea in coastal areas are rare, and they are used for the calibration purpose of wave generation numerical models [4-6].

The change in wind direction from the SE to SW, or vice versa, is a frequent transition occurrence in the region of Kvarner and the Bay of Rijeka. During these transitions, a wave height rise is evident in front of the main breakwater of the Rijeka port (in the vicinity of the V1 reference position, see Figure 1). A wind transition from the SE to SW goes through the SSE and S directions, which have a longer effective fetch length. According to the data presented in [7], the effective fetch lengths for wind directions at the Zagreb pier in the port of Rijeka (currently under construction) are 18 km for SE, 21 km for SSE, 24 km for S, and 20 km for SW (calculated according to [8]). If the wind direction transition is slow, with no change in wind velocity, there will be an increase in wave height during the passage of wind through the sector SSE-SW. The next chapter provides results of the numerical simulation as confirmation of this statement.

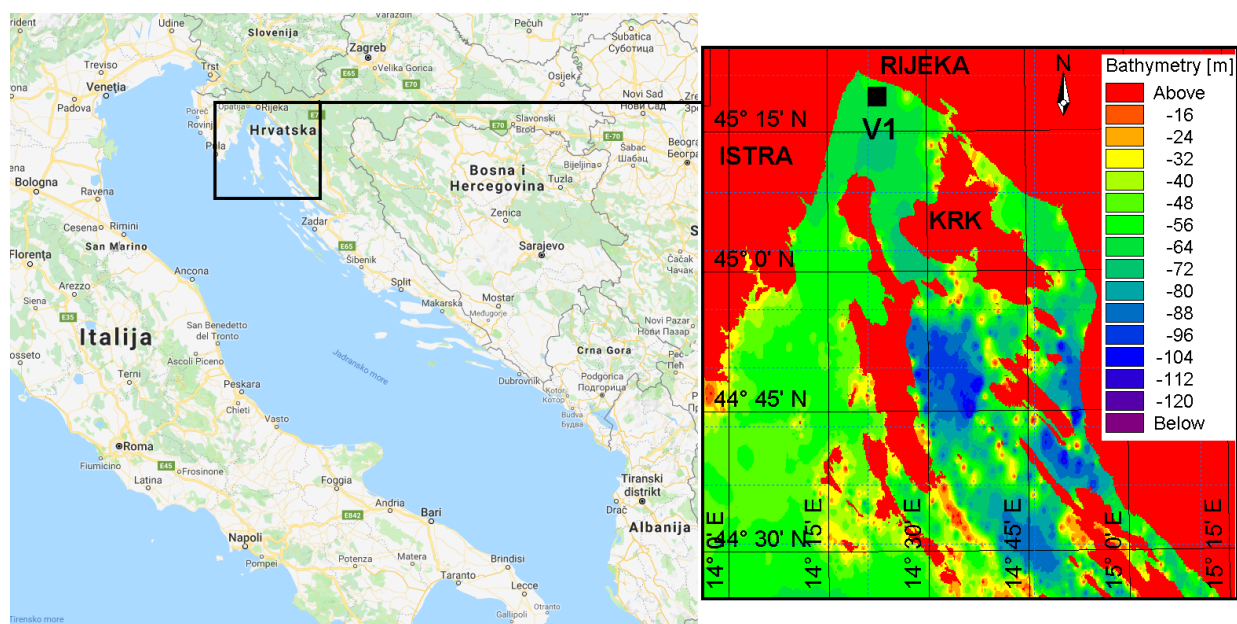


Figure 1 An overview map of the Adriatic Sea area (left) and Kvarner (right) with the location of reference point V1 in front of the port of Rijeka ( $\varphi = 45.3272$ ,  $\lambda = 14.39413$ )



## 2 MATERIALS AND METHODS

### 2.1 The influence of change in wind direction on waves

Three factors affect the growth of wind waves: wind velocity, wind duration, and fetch. In the case of limited fetch, such as in the case of the eastern Adriatic channel system, it is necessary to define an effective fetch length, for example according to the methodology presented in [8]. If the effective fetch length and wind velocity are unchanged, the wind direction change will result in a wave height decrease, with the intensity dependent on the speed of the direction change. Numerical simulation of wave generation on a semicircular domain of 25-km-radius and a constant depth of 50 m (Figure 2) were performed as a contribution to that statement. The model spatial domain was discretized with triangular non-overlapping cells (finite volumes) and appertain nodes located at the center of each individual cell. The model boundaries were closed and nonreflective (wave energy absorbing). In this case, the fetch lengths for point A from the SE, S, and SW wind directions were the same (25 km). In the case of wind transition from the SE to SW direction, the change of wave height at position A depends on the speed of the direction change. Figure 2 shows the evolution of the significant wave height ( $H_S$ ) at point A in cases where the wind direction changes from the SE to SW during 2 and 8 h at a constant wind velocity of 18 m/s. The results from Figure 2 indicate a very slight decrease of  $H_S$  when the wind changes direction (SE  $\rightarrow$  SW) over 8 h, and an  $H_S$  change of approximately 0.2 m in of 2 h of transition.

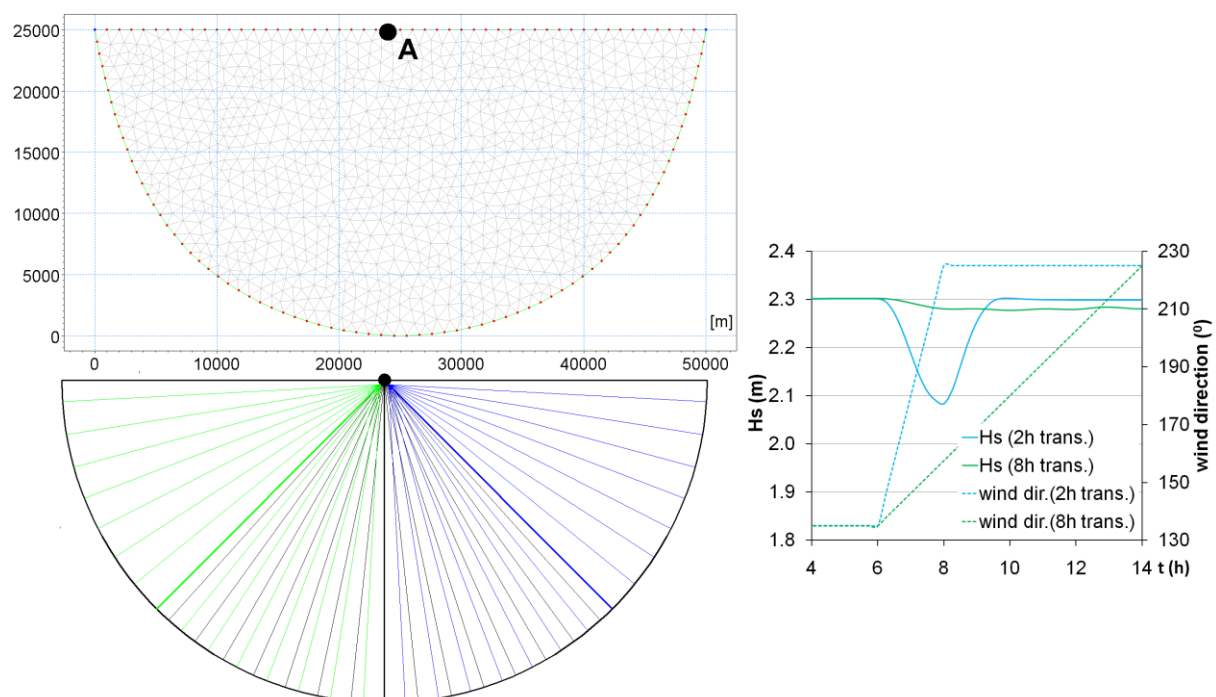


**Figure 2** Spatial discretization of the hypothetical semicircular model domain (top left), the hypothetical domain with drawn lines for the determination of the effective fetch for the SE direction (blue lines), S direction (black lines), and SW direction (green lines) according to the methodology presented in [8] (bottom left), and corresponding significant wave height ( $H_S$ ) at point A during the transition period (right)

If the effective fetch length changes during wind transition SE  $\rightarrow$  SW (Figure 3,  $F_{\text{eff(SE)}} = F_{\text{eff(SW)}} = 15$  km;  $F_{\text{eff(S)}} = 25$  km),  $H_S$  will also develop accordingly. When the transition period is long enough, the longest fetch length through the S direction would be realized. For example, with a transition of 8 h and wind velocity of 14 m/s,  $H_S$  increases by 7.5%. In the case of a transition of 2 h there is also a decrease and increase of  $H_S$  (Figure 3). The results of the simulations suggest that the occurrence of the maximum wave height at V1 should be expected in situations with a slower transition in the wind direction SE  $\rightarrow$  SW.

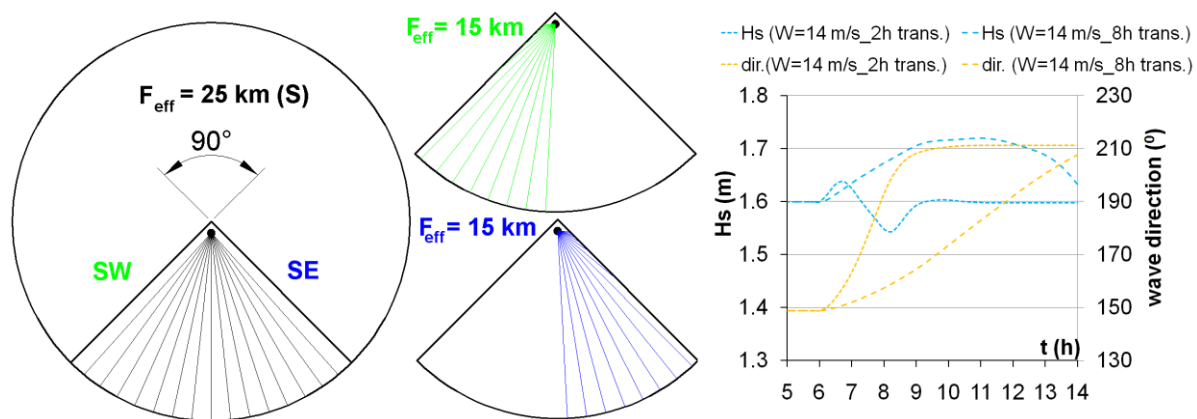


**Figure 3** Rays for the calculation of the effective fetch at the starting wind direction SE (blue lines), end wind direction SW (green lines), and intermediate wind direction S (black lines) and the corresponding significant wave height ( $H_s$ ) at point A during transition periods of 2 and 8 h with a wind velocity of 14 m/s (right)

## 2.2 Initial numerical simulations for the analyzed area (homogenous wind field)

Initial numerical simulations were conducted to confirm the hypothesis about the rise of significant wave heights during the transition period of the wind direction in the analyzed area. Simulations include a series of hypothetical scenarios with the following features:

- during the first 12 h of the simulation period, the homogenous and stationary fields of the SSE direction wind exist. Wind velocities are 6, 10, 14, and 18 m/s;
- after 12 h the transition period begins (variable durations of 2, 4, 6, 8, 10, and 12 h) until new stationary conditions with the SW wind direction are achieved;
- the wind direction is homogeneous throughout the spatial domain and the wind velocity is stationary throughout the simulation period.

Figure 4 shows the spatial domain of the wave generation numerical model. In spatial discretization, non-overlapping triangular cells were used (finite volumes, Figure 4). The distance between the numerical nodes, located at the center of each finite volume, was variable and ranged from 7500 m in the deep-water area to 200 m in the coastline zone. The analyzed area is characterized by a large bathymetric gradient in the coastal zone, and thus wave deformation in the shallow water area was not essential for the wave generation process. Therefore, the applied calculation step was rational.

For the implementation of the numerical simulations, a spectral model of wave generation and wave deformation Mike 21sw ([www.dhigroup.com](http://www.dhigroup.com)) was used. This model relies on spectral formulation according to [9-13] where the spectral frequency domain is discretized by a logarithmic scale with a minimum frequency of 0.08 Hz (wave period = 12.5 s) and maximum frequency of 0.95 Hz (wave period = 1.05 s) through 28 discrete steps. The model routines are based on processes of wind wave generation, mutual nonlinear wave interaction, refraction, diffraction, and white capping (surface wave breaking process). The dissipation processes caused by bottom friction and waves breaking in shallow water are not considered [14]. Numerical integration for the source member was carried out according to the methodology presented in [15].



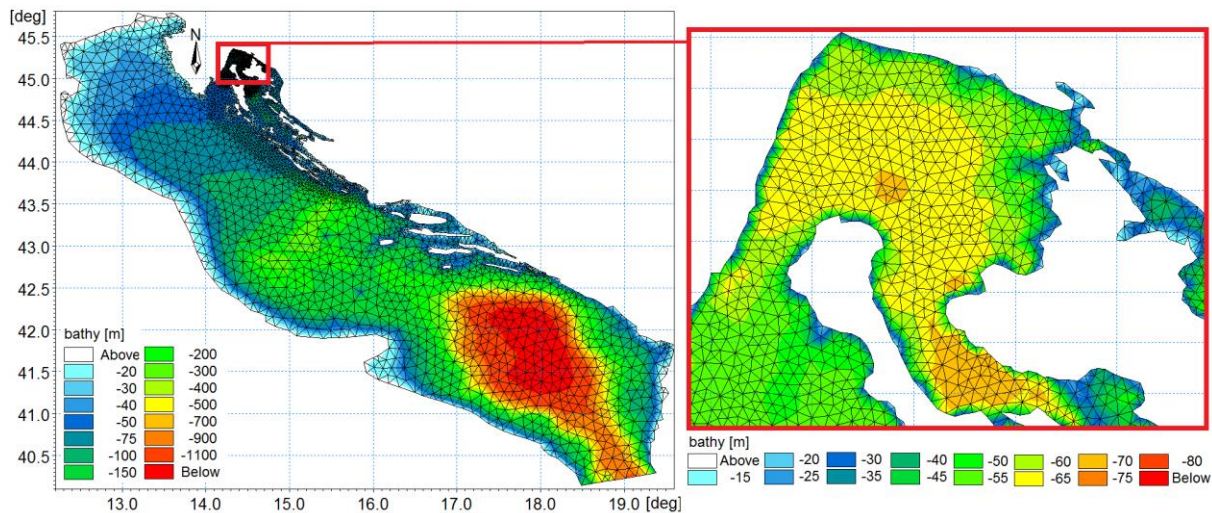


**Figure 4 Spatial discretization of the model domain with the unstructured mesh of finite volumes on the bathymetric background**

Modal parametrization, primarily related to white capping [16], was adopted on the basis of the measured significant wave heights ( $H_s$ ) and peak periods ( $T_p$ ) in conditions of near stationary wind intensity ( $V_{wind} = 6, 10, 14,$  and  $18$  m/s) from the SSE direction after 12 h of continuous activity [17] (Figure 5). At the open boundary, a zero spectrum was used (no wave energy flux through it). This formulation of the boundary conditions excluded the influence of wave generation in the zone of the Mediterranean Sea on waves in the spatial domain of the model (Adriatic Sea, Figure 4), and the results of the numerical analysis are not reliable only in the vicinity of the Otrant strait. The initial conditions were defined by the absence of waves throughout the modelled area.

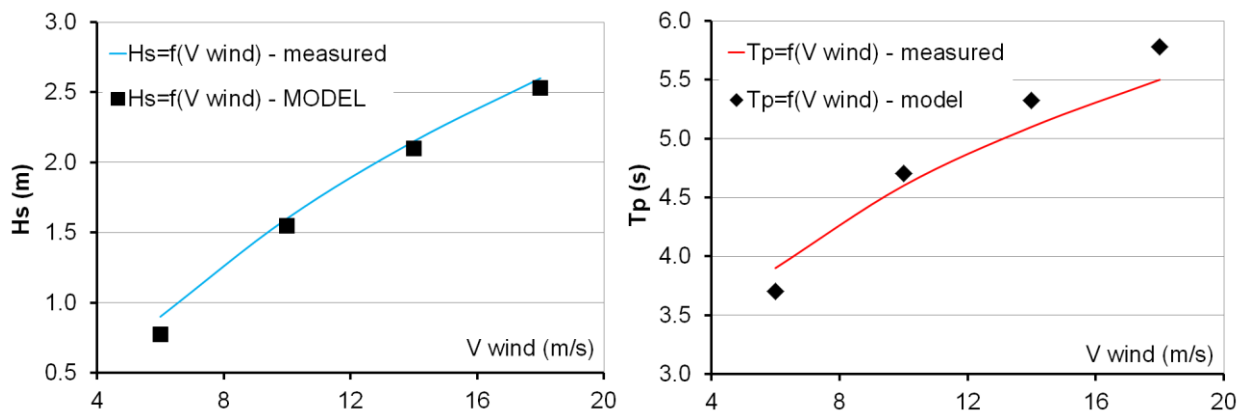


**Figure 5 Measured/modelled significant wave heights ( $H_s$ ) and peak periods ( $T_p$ ) depending on the measured wind velocities from the SSE direction for a duration of 12 h (Rijeka Port main breakwater, [17])**

Post simulation cycles for model parametrization purposes, calculations were performed with the variation of the above-mentioned parameters (wind velocity and transition period, chapter Results).

### 2.3 Application of the wind field from the Aladin-HR model (1998-2001)

During the analyzed periods, the wind field from the Aladin-HR atmospheric model was used with a 4-km-spatial resolution and a time resolution of 3 h [18-20]. From the entire data set, only those situations that have the following characteristics were selected:

- The wind field during the transition is approximately homogeneous, the wind direction change SSE → SW generally occurs throughout Kvarner and the Bay of Rijeka;



- The initial wind direction at the V1 position and the position of the reference point in front of the entrance to Kvarner (open sea, Figure 7) is in the range ESE (112.5°) - S (180°);
- At the position of the reference point in front of the Kvarner entrance, the wind direction changes through the transition period to the "final" direction in the range SSW (202.5°) - WSW (247.5°). The angle of the wind direction is continuously increasing during the transition period;
- The "final" wind direction angle at the position V1 is greater than the initial one;
- At the position V1 the minimum wind velocity is 4 m/s, while at the reference point in front of the Kvarner entrance the minimum wind velocity is 7 m/s;
- The maximum deviation of the wind velocity through the transition period is  $\pm 25\%$  of the initial value.

The beginning of a particular situation, its duration, directions, and velocities of the wind are shown in Table 1. Extracting the results from the Aladin-HR model for the period 1998–2001, it is possible to identify a total of 4 situations that meet the above-mentioned criteria. For all situations listed in Table 1, numerical wave generation simulations were performed using the model spatial domain shown in Figure 2 (shown in the next chapter).

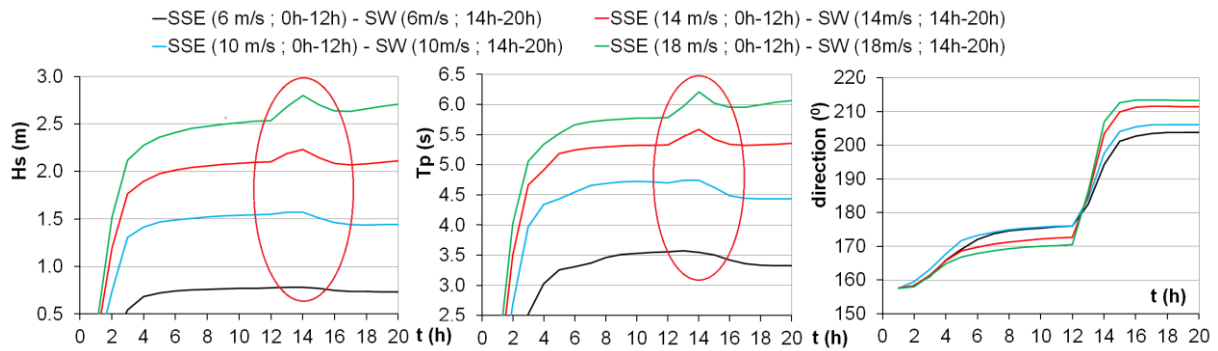
**Table 1 The beginning of a particular situation, wind direction ( $\alpha_0$ ), and wind velocity ( $V_0$ ) at the start of transition; wind direction ( $\alpha_{+3}$ ) and wind velocity ( $V_{+3}$ ) after 3 h of transition; wind direction ( $\alpha_{+6}$ ) and wind velocity ( $V_{+6}$ ) after 6 h of transition; transition duration ( $T$ ) (extraction of the results from the Aladin-HR model for the period 1998-2001)**

Situation	Beginning of the situation	Parameters in front of the entrance to the Kvarner									
		$\alpha_0$ (°)	$\alpha_{+3}$ (°)	$\alpha_{+6}$ (°)	$\alpha_{+9}$ (°)	$V_0$ (m/s)	$V_{+3}$ (m/s)	$V_{+6}$ (m/s)	$V_{+9}$ (m/s)	$T$ (h)	$\Delta H_S$ (m)
1	7/4/1998 18:00	178	196	218	225	7.6	9.1	9.2	7.8	9	+0.13
		183	184	189	202	4.7	5.2	5.0	3.6		
2	28/12/1999 3:00	178	214	-	-	14.9	13.3	-	-	3	+0.67
		162	200	-	-	9.0	8.5	-	-		
3	12/4/2000 0:00	176	187	198	208	7.2	7.1	8.6	9.0	9	+0.22
		168	173	183	186	4.8	4.9	6.0	5.9		
4	2/3/2001 18:00	141	177	221	-	11.5	12.0	9.8	-	6	+0.28
		173	161	183	-	6.3	6.8	5.6	-		

### 3 RESULTS

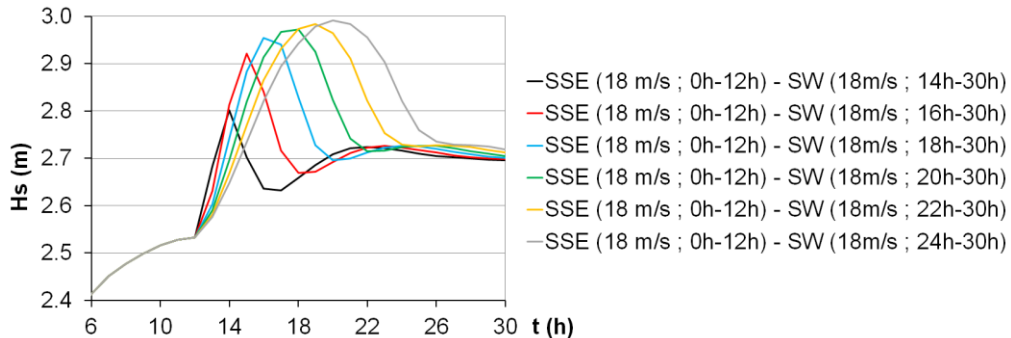
Figure 6 shows the time series of significant wave height ( $H_S$ ), peak period ( $T_P$ ), and incident wave direction for position V1 (Figure 1) in the case of wind velocity variation (6, 10, 14, and 18 m/s) and for the same transition period of 2 h (from 12 to 14 h of the simulation, homogenous wind field – initial numerical simulations).

Figure 6 indicates the occurrence of the maximum values of  $H_S$  and  $T_P$ . It is observed that higher wind velocities generate more distinct  $H_S$  and  $T_P$  values. At wind velocities of 6 m/s, these maximum values do not appear.



**Figure 6** Time series of the significant wave heights ( $H_s$ ), peak periods ( $T_p$ ), and incident wave direction for position V1 with variation of wind velocity and uniform transition period (2 h, 12 to 14 h simulation)

Figure 7 shows the development of significant wave height ( $H_s$ ) at the position V1 (Figure 1) during transition periods with variable duration (from 2 to 12 h) and stationary wind velocity of 18 m/s (homogenous wind field – initial numerical simulations). From Figure 7, it is apparent that longer transition period result in more obvious  $H_s$  maximums.



**Figure 7** Development of significant wave height ( $H_s$ ) at position V1 during transition periods with variable duration (from 2 h to 12 h) and stationary wind velocity of 18 m/s

Figure 8 shows model  $H_s$  fields in the case of a homogenous wind field with a velocity of 18 m/s at the beginning of wind direction transition (12<sup>th</sup> hour of simulation, SSE wind), at the middle of the transition period (15<sup>th</sup> hour of simulation, S wind) and at the end of the transition period (18<sup>th</sup> hour of simulation, SW wind).

The results presented in Figure 8 clearly show the occurrence of the largest wave heights when the wind is passing through the S direction, as a result of reaching the maximum effective fetch length. Further progress of the wind towards the SW direction reduces the fetch length, which results in the wave height decreasing.

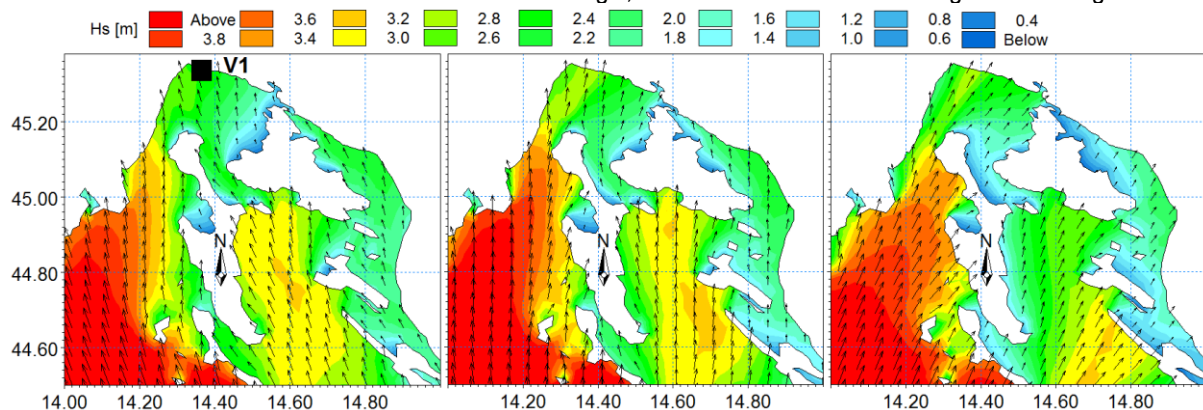


**Figure 8** Model  $H_s$  fields in the case of a homogenous wind field with a velocity of 18 m/s and transition period from 12 to 18 h of simulation (left – 12<sup>th</sup> hour simulation, SSE wind; middle – 15<sup>th</sup> hour simulation; right – 18<sup>th</sup> hour simulation, SW wind)





Figures 9-11 show the wind fields from the Aladin-HR model along with the corresponding  $H_s$  fields gained from the wave generation model for the beginning and end of situations 1 - 4 from Table 1. Figure 12 shows the time course of significant wave height ( $H_s$ ) at position V1 for the situations given in Table 1.

In situations 1 and 3, the average wind velocities during the transition period are similar (8.4 and 8.0 m/s, respectively, at the reference point in front of the Kvarner entrance, 4.6 m/s and 5.4 m/s, respectively, at position V1), and thus the increase of the  $H_s$  has a similar trend. According to the results obtained from the initial numerical simulations, under the homogeneous wind field with a velocity of 6 m/s, the increase of  $\Delta H_s$  is practically absent (Figure 6). Therefore, it can be concluded that most of the increase in the significant wave heights in situation 1 ( $\Delta H_s = +0.13$  m) and 3 ( $\Delta H_s = +0.22$  m) is generated by the wind velocity increase during the transition period.

The most prominent increase in  $\Delta H_s$  was achieved in situation 2, where the highest mean wind velocity occurs during the transition (14.1 m/s at the reference position in front of the Kvarner entrance, 8.8 m/s at site V1).  $\Delta H_s$  at position V1 is +0.67 m and  $H_s$  at the end of the transition period is 1.9 m. This  $H_s$  value is consistent with the results obtained from the initial simulations (Figure 6).

In situation 4 during the first 4 h of wind transition, a continuous increase of  $H_s$  occurs, and from 4 to 6 h of transition  $H_s$  falls slightly because of the wind velocity decreasing in the entire region of Kvarner and Rijeka Bay. The mean wind velocities during the transition period were 11.1 m/s at the reference point in front of the Kvarner entrance and 6.2 m/s at the V1 position. These values are in-between the mean wind velocities from situations 2 and 3, and the increase of  $H_s$  ( $\Delta H_s = +0.28$  m) is in-between the  $\Delta H_s$  values obtained in situations 2 and 3.

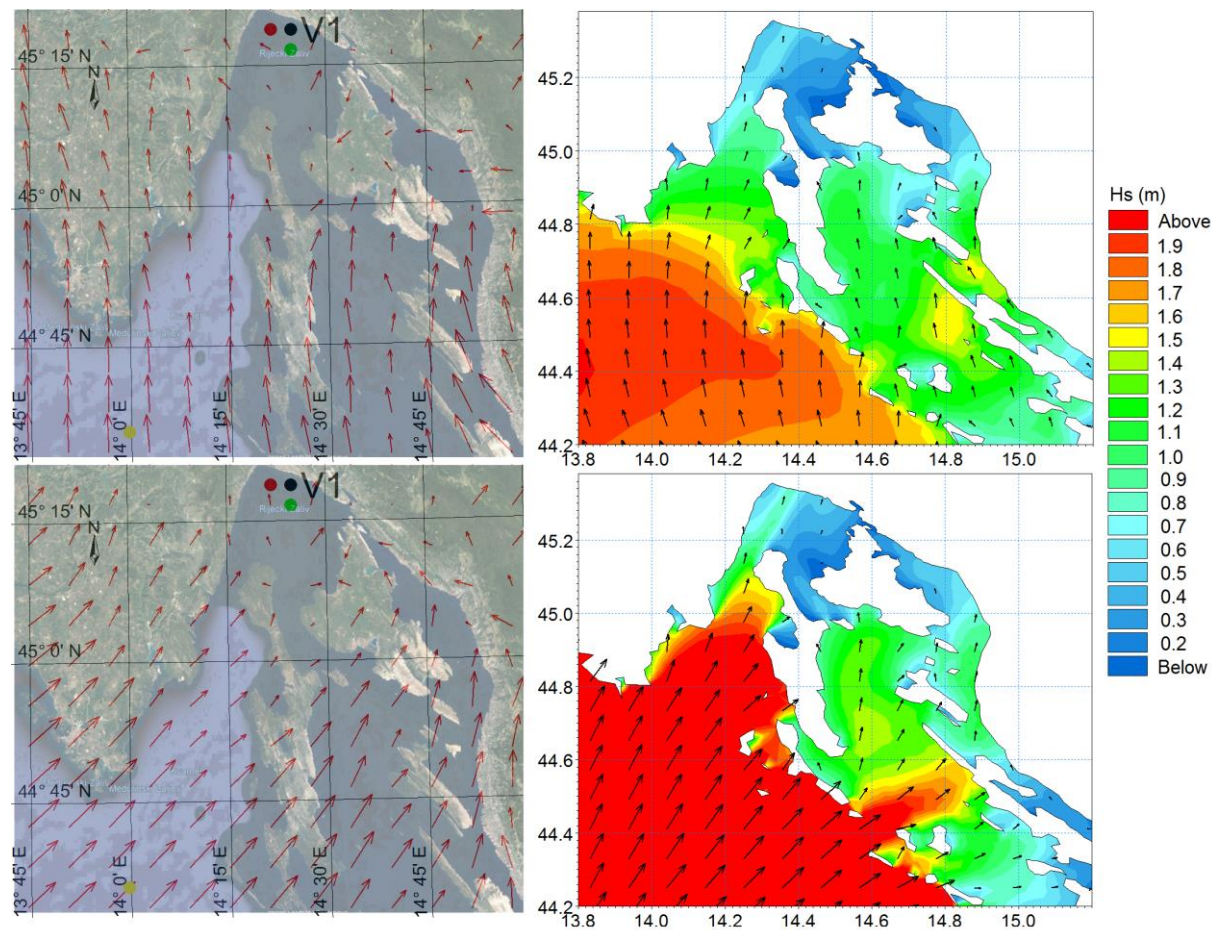


Figure 9 The wind field (model Aladin-HR, left) and corresponding  $H_s$  field (wave generation model, right) at the beginning (top) and the end (bottom) of transition situation 1

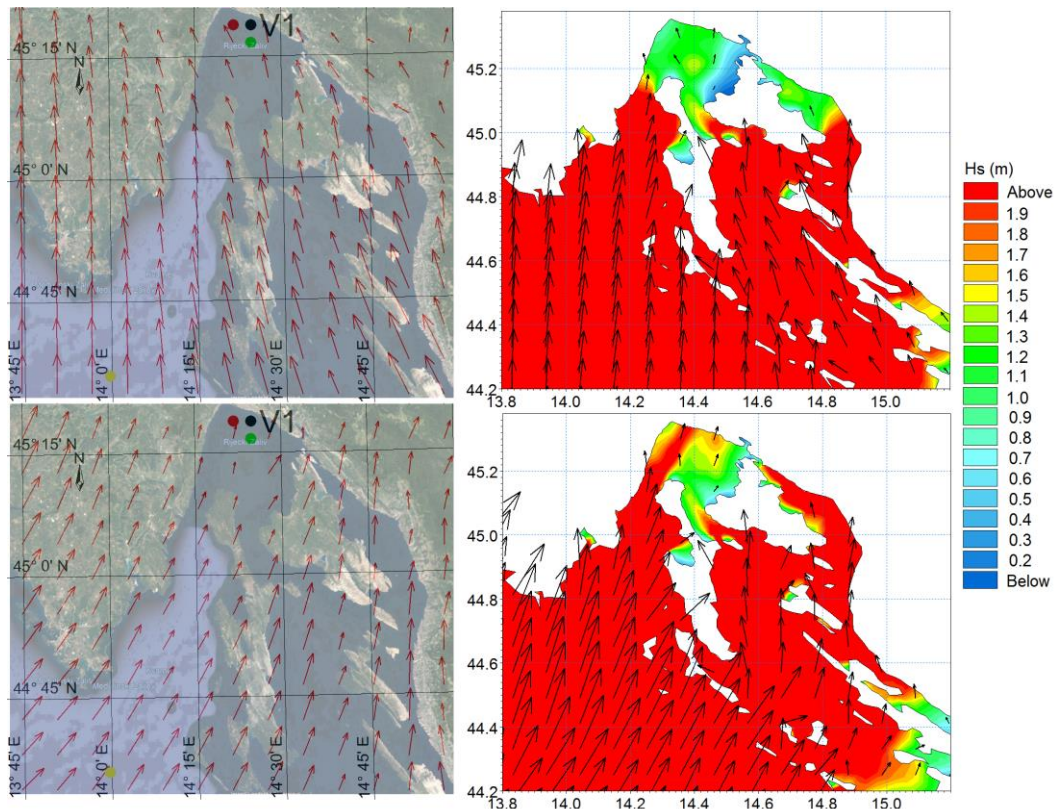


Figure 10 The wind field (model Aladin-HR, left) and corresponding  $H_s$  field (wave generation model, right) at the beginning (top) and the end (bottom) of transition situation 2

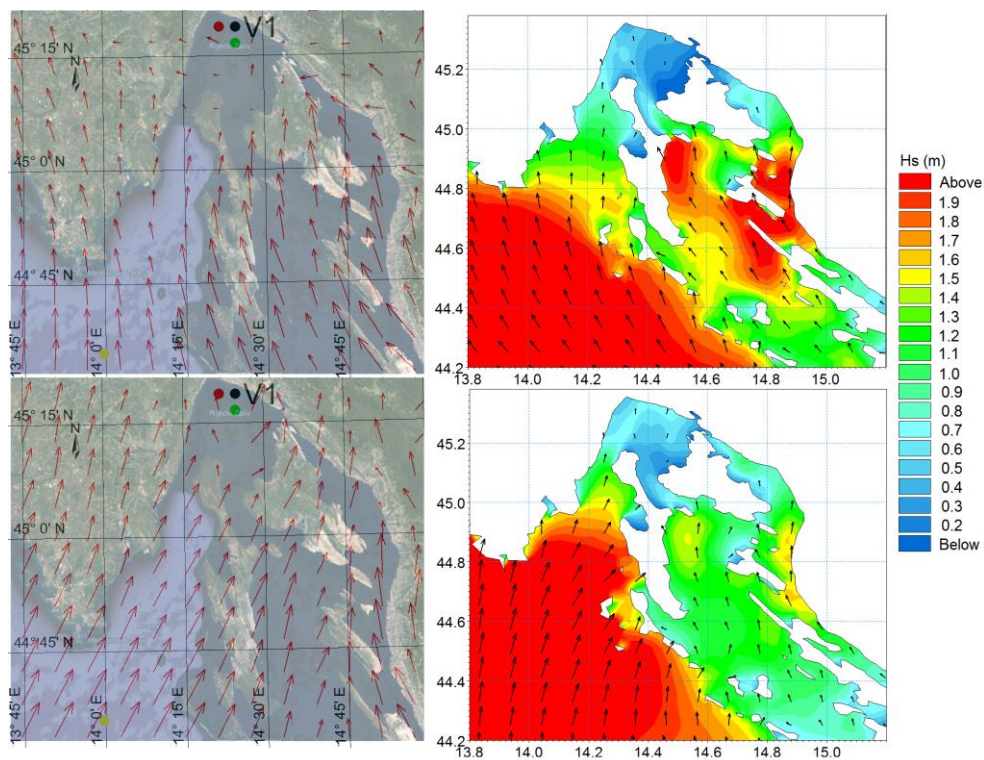


Figure 11 The wind field (model Aladin-HR, left) and corresponding  $H_s$  field (wave generation model, right) at the beginning (top) and the end (bottom) of transition situation 3



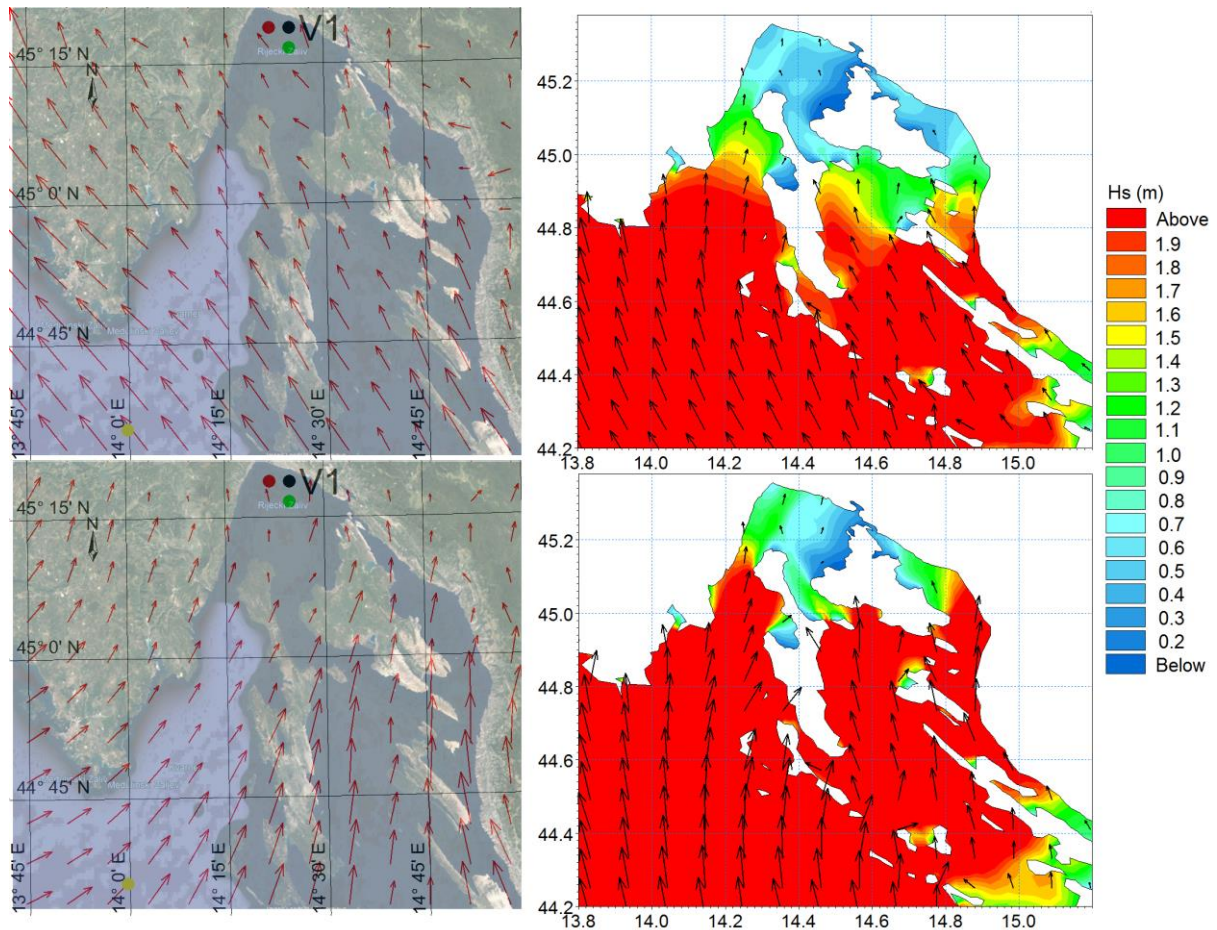


Figure 12 The wind field (model Aladin-HR, left) and corresponding  $H_s$  field (wave generation model, right) at the beginning (top) and the end (bottom) of transition situation 4

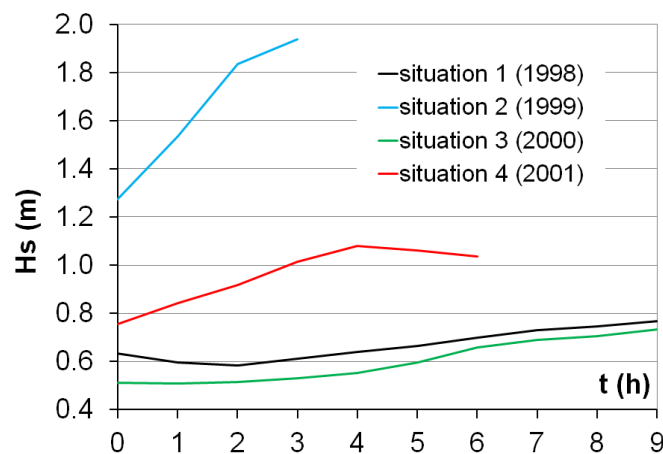


Figure 13 The development of the significant wave height ( $H_s$ ) at position V1 for the situations given in Table 1

The approximate ratio of the mean wind velocities during the transition period, also averaged for the V1 position and the reference point in front of the Kvarner entrance ( $V_{AV} - transition$ ), and the increase of the significant wave height  $\Delta H_s$  are shown in Figure 14.

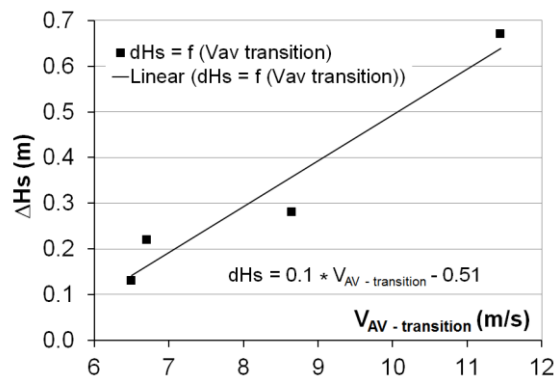


Figure 14 Approximate ratio of the mean wind velocities during the transition period ( $V_{AV-transition}$ ) and increase of the significant wave height  $\Delta Hs$

#### 4 DISCUSSION

Regarding the reliability of the data from the Aladin-HR model, it should be noted that the velocity field in the Rijeka bay is extremely inhomogeneous in direction and intensity, as documented in Figure 15. Figure 15 shows the wind roses for three adjacent numerical nodes in the Aladin-HR model (see Figures 9-12, the black circle - the numerical node for position V1, the red circle - the first numerical node to the left of the position V1, and the green circle - the first numerical node below position V1). The wind roses are given only for the year 2001. The numerical models of wind generation are forced by the result of the atmospheric numerical model (Aladin-HR in case of this study) that has a prognostic character and usually forecasts extreme wind velocity and direction changes only with limited accuracy [21]. With the progress of computation possibilities and resources strong improvements can be expected with regards to the reliability of calculated wind fields from atmospheric models. For example, a new set-up of the Aladin-HR model based on a finer calculation grid (spatial resolution of 2 km) that is capable of resolving relevant variability in the wind field, even with the complex Adriatic coastal morphology.

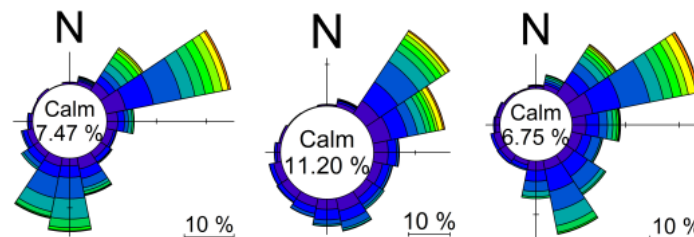


Figure 15 Wind roses for three adjacent numerical nodes in the Aladin-HR model, for the year 2001 (left - the numerical node for position V1, middle - the first numerical node to the left of position V1, and right - the first numerical node below position V1)

It should be mentioned that the analyses were not conducted with the aim of finding and commenting on situations in which the maximum wave height at position V1 appears. That is, the maximum wave height at V1 is achieved under conditions of a relatively homogeneous wind field with a SE/SEE direction across the entire Adriatic basin. An example of the significant wave height development in such a situation is given in Figure 16 (6/11/2000 12:00 - 21:00).

The presented results of the model simulations in this paper have not been verified by in-situ measurements. Although a relatively scarce data pool on measured wave parameters within the eastern Adriatic channel system is available, the general difference between the wave spectra evolution in the open sea and the semi-enclosed channel system is recognized. During the wind velocity increase in the Adriatic open sea area, the spectral wave energy increases and reaches its maximum. Simultaneously, the maximum of the spectrum moves toward higher periods. During the period of wind velocity decrease the spectral energy also decreased, while the spectrum maximum moves further toward the lower frequencies [22]. In the semi-enclosed area, evolution of the





wave spectra differ significantly, mainly in the period of decreasing wind velocity when the spectrum maximum is shifted considerably in time toward the higher frequencies [22].

According to the study results presented in [23], wave heights will increase in areas such as parts of Indonesia, the Southern Ocean and Australia's east coast. On the other hand, a decrease in wave height for more than one-quarter of the world's oceans is to be expected, particularly in the Northern Hemisphere. Accordingly, climate change is not a relevant concern regarding the analyzed phenomena in the study area.

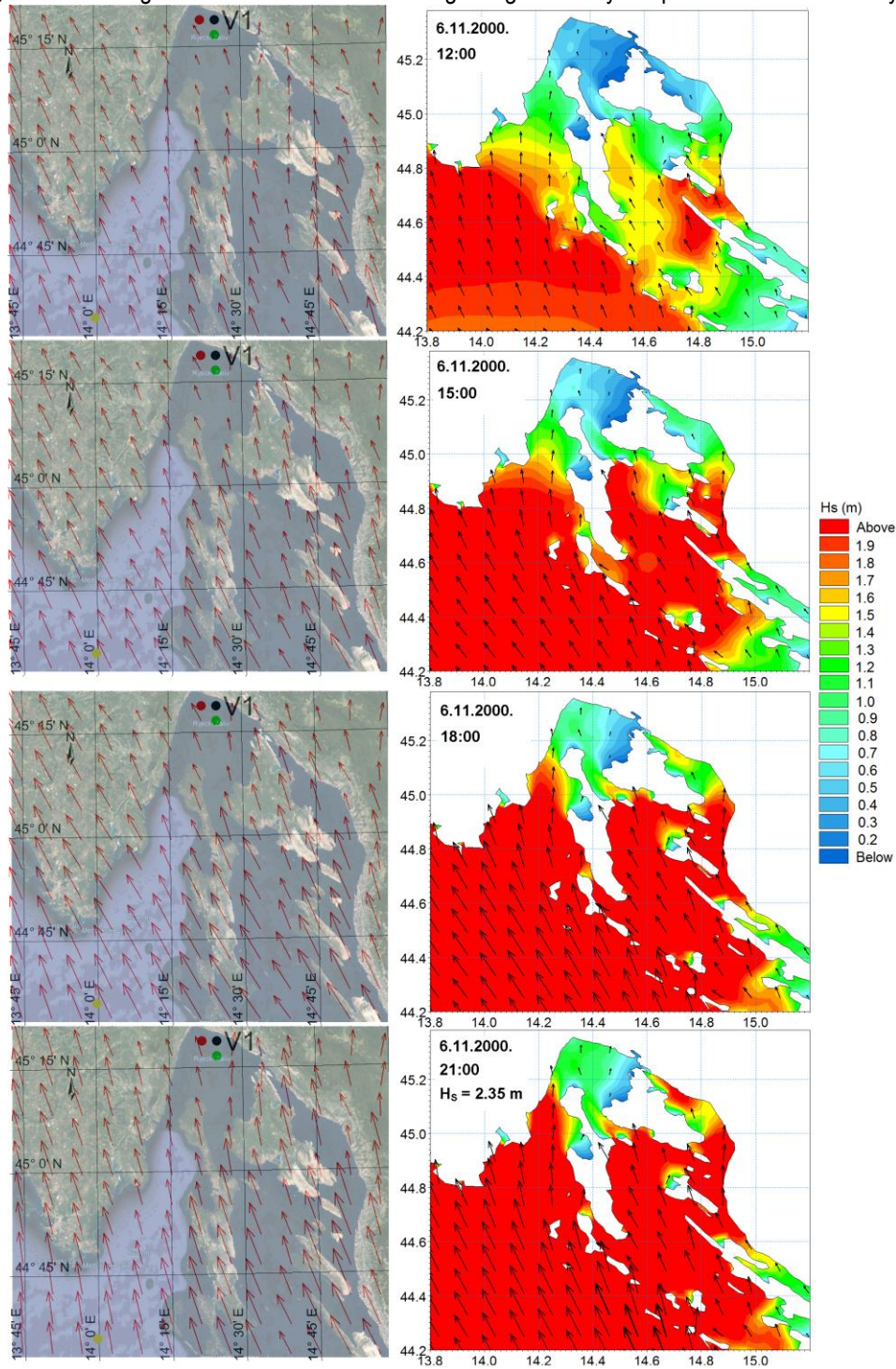


Figure 16 Significant wave height fields in the situation of a relatively homogenous wind field with a SE/SEE direction across the entire Adriatic basin (6/11/2000 12:00 - 21:00)





## 5 CONCLUSION

A numerical analysis of significant wave height dynamics in the deep-water area in front of the Rijeka port has been conducted for the scenario of a wind direction transition from SE to SW. The numerical model domain covers the entire Adriatic basin, and some relevant situations from the period 1998-2001 were analyzed. The numerical model was forced by the wind field obtained from the atmospheric model Aladin-HR.

The results of the analyses show that an increase of  $H_s$  occurs only in situations where a wind transition from SSE → SW takes place in the wider area of Kvarner. An increase in wind velocity results in a more noticeable increase of  $H_s$  in the transition period.

The ratio of the mean wind velocity during the transition period and the increase of the significant wave height for the deep-water area in front of the port of Rijeka were defined according to the results of numerical simulations.

Data analysis of the wind velocity and direction obtained by the Aladin-HR atmospheric model indicate the requirement for finer spatial resolution data due to distinct spatial variability in the wind field.

Further research will follow after obtaining wind field data from the Aladin model for the more recent period, i.e., 2001 - 2016.

## References:

- [1] Andročec, V. et al. 2009: The Adriatic Sea Monitoring Program, Final Report, Ministry of environmental protection, physical planning and construction of the Republic of Croatia, Zagreb (in Croatian)
- [2] Smirčić, A.; Gačić, M. 1983: Spatial and temporal characteristics of surface waves in the Adriatic Sea caused by extremely strong SE wind, Hidrografski godišnjak 1978-1979, pp. 17-22, (In Croatian)
- [3] Leder, N.; Smirčić, A.; Vilibić, I. 1998: Extreme values of surface wave heights in the northern Adriatic, Geofizika, 15, pp. 1-13.
- [4] Lončar, G.; Ocvirk, E.; Andročec, V. 2010: Usporedba modeliranih i mjerenih površinskih vjetrovnih valova, Građevinar, 62 (3), pp. 45-55. (in Croatian)
- [5] Lončar, G.; Leder, N.; Paladin, M. 2012: Numerical modelling of an oil spill in the northern Adriatic, Oceanologia, 54 (2), pp. 143-173, <https://doi.org/10.5697/oc.54-2.143>
- [6] Bartolić, I.; Lončar, G.; Bujak, D.; Carević, D. 2018: The Flow Generator Relations for Water Renewal through the Flushing Culverts in Marinas, Water, 10 (7), pp. 1-22, <https://doi.org/10.3390/w10070936>
- [7] Hydroexpert 2013: Wind and wave climate for the Port of Rijeka – Zagreb pier, 30 p.
- [8] CERC 1984: Shore protection Manual, Vol I, 2nd edition, US Army Corps of Engineers - Coastal Engineering Research Center, Washington D. C.
- [9] Janssen, P. A. E. M. 1989: Wave induced stress and drag of airflow over sea waves, Journal of Physical Oceanography, 19, pp. 745-754, [https://doi.org/10.1175/1520-0485\(1989\)019<0745:WISATD>2.0.CO;2](https://doi.org/10.1175/1520-0485(1989)019<0745:WISATD>2.0.CO;2)
- [10] Janssen, P. A. E. M. 1991: Quasi-linear theory of wind wave generation applied to wave forecasting, Journal of Physical Oceanography, 21, pp. 1631-1642, [https://doi.org/10.1175/1520-0485\(1991\)021<1631:QLTOWW>2.0.CO;2](https://doi.org/10.1175/1520-0485(1991)021<1631:QLTOWW>2.0.CO;2)
- [11] Janssen, P. A. E. M. 1992: Experimental evidence of the effect of surface waves on the airflow, Journal of Physical Oceanography, 22, pp. 1600-1604, [https://doi.org/10.1175/1520-0485\(1992\)022<1600:EEOTEO>2.0.CO;2](https://doi.org/10.1175/1520-0485(1992)022<1600:EEOTEO>2.0.CO;2)
- [12] Janssen, P. A. E. M. 1998: On the effect of ocean waves on the kinetic energy balance and consequences for the initial dissipation technique, Journal of Physical Oceanography, 30, pp. 1743-1756, [https://doi.org/10.1175/1520-0485\(1999\)029<0530:OTEOWW>2.0.CO;2](https://doi.org/10.1175/1520-0485(1999)029<0530:OTEOWW>2.0.CO;2)
- [13] Komen, G.J.; Cavaleri, M.; Donelan, K.; Hasselmann, S.; Hasselmann, K.; Janssen, P. A. E. M. 1994: Modelling of dynamic of ocean surface waves. Cambridge university press, Cambridge, 532 p.
- [14] Johnson, H. K. 1998: On modelling wind-waves in shallow and fetch limited areas using method of Holthuijsn, Booij and Herbers, Journal of Coastal Research, 14(3), pp. 917-932.
- [15] Herzbach, H.; Janssen, P. A. E. M. 1999: Improvement of the short-fetch behaviour in the Wave Ocean Model (WAM), Journal of Atmospheric and Oceanic Technology, 16, pp. 884-892, [https://doi.org/10.1175/1520-0426\(1999\)016<0884:IOTSFB>2.0.CO;2](https://doi.org/10.1175/1520-0426(1999)016<0884:IOTSFB>2.0.CO;2)



- [16] Kahma, K. K.; Calkoen, C. J. 1992: Reconciling discrepancies in the observed growth of wind-generated waves, *Journal of Physical Oceanography*, 22(12), pp. 1389-1405, [https://doi.org/10.1175/1520-0485\(1992\)022<1389:RDITOG>2.0.CO;2](https://doi.org/10.1175/1520-0485(1992)022<1389:RDITOG>2.0.CO;2)
- [17] Građevinski institut 1991: Hidraulička analiza valova i nasipnih konstrukcija sjeverne obale brodogradilišta 3. Maj u Rijeci, Građevinski institut, (in Croatian)
- [18] Brzović, N. 1999: Factors affecting the Adriatic cyclone and associated windstorms, *Contributions to Atmospheric Physics*, 72, pp. 51-65.
- [19] Brzović, N.; Strelec-Mahović, N. 1999: Cyclonic activity and severe jugo in the Adriatic, *Physics and Chemistry of the Earth (B)*, 24, pp. 653-657, [https://doi.org/10.1016/S1464-1909\(99\)00061-1](https://doi.org/10.1016/S1464-1909(99)00061-1)
- [20] Ivatek-Šahdan, S.; Tudor, M. 2004: Use of high-resolution dynamical adaptation in operational suite and research impact studies, *Meteorologische Zeitschrift*, 13 (2), pp. 99-108, <https://doi.org/10.1127/0941-2948/2004/0013-0099>
- [21] Lončar, G.; Ocvirk, E.; Kunštek, D. 2010: Numerical analysis of significant wave height of 5-year return period in the southern Adriatic, *Tehnički vjesnik-Technical Gazette*, 17 (4), pp. 389-395.
- [22] Leder, N.; Andročec, V.; Čupić, S.; Domijan, N.; Lončar, G. 2010: Evolution of surface wave spectra in extreme sea states along the eastern Adriatic open sea and channel areas, *Rapport du 39e Congres de la CIESM*, Briand, Frederic (ed.), Venice, pp. 135-135.
- [23] Hemer, M. A.; Fan, Y.; Mori, N.; Semedo, A; Wang, X. L. 2013: Projected changes in wave climate from a multi-model ensemble, *Nature Climate Change*, 3, pp. 471-476.

Please cite this article as:

Lončar, G, Šreng, Ž, Miličević, H, Ostojić, S: Increase of wave height due to transition in wind direction - example: Rijeka bay, *Electronic Journal of the Faculty of Civil Engineering Osijek-e-GFOS*, 2019, 18, pp. 57-70, <https://doi.org/10.13167/2019.18.6>